Intermittent Chaos and Low-Frequency Noise in the Driven Damped Pendulum

E. G. Gwinn and R. M. Westervelt
Division of Applied Sciences and Department of Physics, Harvard University, Cambridge, Massachusetts 02138
(Received 6 December 1984)

A study of intrinsic and noise-induced intermittency and low-frequency noise due to crises is reported for numerical simulations of the sinusoidally driven dampled pendulum and radio-frequency–driven Josephson junctions. The effects of fractal boundaries of the basins of attraction on the functional form, noise sensitivity, and noise scaling of low-frequency power spectra are considered.

PACS numbers: 05.45.+b, 05.40.+j, 72.70.+m, 74.50.+r

A fascinating problem in modern dynamics is the origin of qualitative changes in the behavior of nonlinear physical systems on very long time scales and the resulting low-frequency noise. This intermittency is the subject of much current theoretical work on dynamical systems[1–9]; important issues are the different mathematical origins of intermittent chaos and the influence of external noise. A dynamical system which models the interaction of competing periodicities and frequency locking in a wide variety of physical systems is the equation describing the damped driven pendulum. This equation is formally identical to the resistively-shunted-junction (RSJ) model for radio-frequency–driven Josephson junctions. The study of chaos in Josephson junctions has been the focus of recent theoretical[10–20] and experimental[21–24] work; in most cases, the only experimentally observable chaos is intermittency.

In this Letter we report a study of intermittency in numerical simulations of the damped driven pendulum emphasizing the role of the basins of attraction for different stable states of the dynamical system, both in intrinsic and external-noise–induced intermittency. We find that the basin boundaries are fractal sets,[25] and that intrinsic intermittency occurs via a crisis[4,5]: the intersection of a chaotic attractor with an unstable periodic orbit on the basin boundary. The intrinsic low-frequency power spectrum is power law ($1/\omega^{\alpha}$) at the crisis and becomes approximately Lorentzian above; both cases are relatively insensitive to external noise. The fractal dimension of the basin boundaries approaches $d=2$ just below the crisis, and external noise easily induces intermittency.

Pomeau and Manneville (PM) describe three characteristic ways in which intermittent chaos can occur near periodic stable orbits in mathematical dynamical systems without external noise[2]; two are discussed here. Type 1 intermittency is associated with the transition from chaos to a stable periodic orbit via a saddle-node bifurcation. Its qualitative features are irregularly spaced bursts of chaotic noise which separate long, nearly periodic intervals for values of a driving parameter g below the critical value g_c at which the bifurcation occurs. The average laminar time $\bar{\tau}$ scales as[2,3]

$$1/\bar{\tau} \propto |g-g_c|^{1/2} \tag{1}$$

for nearly periodic flows with quasi-one-dimensional return maps. Type 3 intermittency occurs when a trajectory diverges slowly from an unstable periodic orbit at a rate which approaches zero at the orbit; its qualitative features are similar to those of type 1. Both types of intermittency produce large amounts of low-frequency noise, which for type 3 can have an approximately $1/\omega$ power spectrum,[2,6,20] where ω is the frequency.

Grebogi, Ott, and Yorke[4] have considered crises and long-lived chaotic transients which occur in dynamical systems when a stable *chaotic* attractor collides with an unstable orbit on the boundary of the basin of attraction. These crises can produce intermittent switching between separate small-scale metastable chaotic orbits on a very long time scale.[4] The average time $\bar{\tau}$ on each small metastable chaotic attractor for the quasi-one-dimensional case scales as[4]

$$1/\bar{\tau} \propto |g-g_c|^{1/2}, \tag{2}$$

where g and g_c are defined above. We show below that crisis-induced intermittency can produce low-frequency noise with an approximately $1/\omega$ power spectrum at the transition $g=g_c$. Both Pomeau-Manneville and crisis-induced intermittency are present in each periodic window in the chaotic region of the one-dimensional logistic map; for example, PM type-1 intermittency near the saddle-node bifurcation which produces the periodic orbit, and crisis-induced intermittency near the crisis which destroys the banded chaotic attractor.[4]

The equation describing both the damped, sinusoidally driven pendulum and the RSJ model for Josephson junctions given in reduced units[13] is

$$\ddot{\theta}+(1/Q)\dot{\theta}+\sin\theta = g\cos\omega_0 t+\delta g(t), \tag{3}$$

where θ is the pendulum angle, Q is the quality factor, g and ω_0 are the amplitude and angular frequency of the driving torque, and $\delta g(t)$ is a possible external noise term, taken to be $\delta g(t)=0$ unless noted. In order to avoid uncertainties due to noise in analog simu-

lators we solved Eq. (3) on a digital computer using double-precision arithmetic and a fourth-order Runge-Kutta algorithm with numerical precision exceeding thirteen decimal places. The solutions for $\theta(t)$ display a rich variety of periodic, chaotic, and intermittent behavior which is described in detail elsewhere.[10-20]

To study intermittency and low-frequency noise we focused on several sets of parameter values for which $\theta(t)$ has running modes in which the angular velocity $\dot{\theta}(t)$ has an average positive or negative dc component. These running modes, produced by symmetry breaking,[13] correspond to positive and negative zero-current voltage steps in an rf-driven Josephson junction. For parameter values $\omega_0 = \frac{2}{3}$, $Q = 2$, and $g \lesssim 1.5$, for example, two separate stable periodic running modes exist with dc angular velocity $\dot{\theta} = \frac{2}{3}\omega_0$. As g increases these modes become chaotic, yet remain separate. At a critical value $1.4954 < g_c < 1.4955$ intermittent switching between positive and negative average-angular-velocity modes occurs on a very long time scale. This intermittency is intrinsic and occurs without added external noise [$\delta g(t) = 0$].

The qualitative nature of this intermittent switching is shown in the phase portrait $\dot{\theta}$ vs θ in Fig. 1(a) for $g = 1.5000$, where the orbit irregularly switches between positive and negative directions. This intrinsic intermittency is induced by small-scale chaotic fluctuations present in both modes. Two low-frequency power spectra $S_{\dot{\theta}^2}(\omega)$ are shown in Figs. 1(b) and 1(c), one at $g = 1.4955$, just above the transition, in Fig. 1(b), and one for $g = 1.5000$ in Fig. 1(c). Because the dc component of angular velocity in the two running modes is not zero, intermittent switching between modes produces large amounts of noise at frequencies ω less than the driving frequency ω_0. Just at the transition $g = g_c$ the noise has an approximately $1/\omega$ power spectrum over more than two decades in frequency ω as shown in Fig. 1(b). At higher g a knee occurs at a low frequency, and the noise spectrum resembles a Lorentzian as shown in Fig. 1(c), which represents typical behavior.[11] The qualitative nature of the transition to intermittency illustrated in Fig. 1, small-scale chaos to intermittent chaos, is not described by any of the Pomeau-Manneville types,[2] but is in agreement with crisis-induced intermittency as described by Grebogi, Ott, and Yorke.[4]

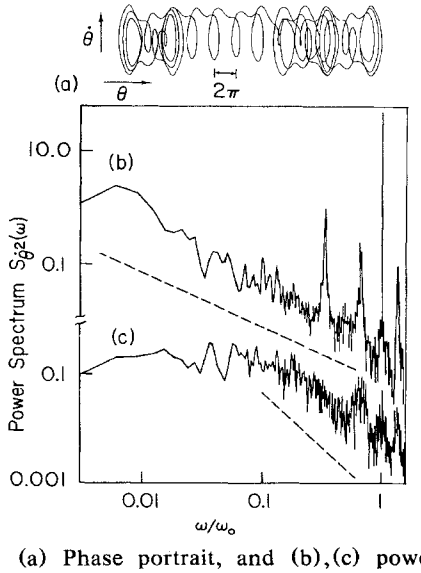

FIG. 1. (a) Phase portrait, and (b),(c) power spectra computed from Eq. (3) without added noise; parameter values $\omega_0 = \frac{2}{3}$; $Q = 2$; (a) and (c) $g = 1.5000$; (b) $g = 1.4955$. Dashed lines of logarithmic slope -1 and -2 are provided for reference.

In order to investigate further the nature of the transition to intermittency, we computed the basins of attraction in θ and $\dot{\theta}$, shown in Fig. 2, for the positive and negative stable or metastable running modes at several values of g: far from the crisis for $g = 1.4600$ and $g = 1.4800$ in Figs. 2(a) and 2(b) where the running modes have dc angular velocity $\dot{\theta} = \omega_0$, and near the crisis, on either side, for $g = 1.4954$ and $g = 1.4955$ in Figs. 2(c) and 2(d). To compute Fig. 2, pairs of initial conditions θ and $\dot{\theta}$ at $\omega_0 t = 0$ were chosen on a grid spanning $0 < \theta < 2\pi$ and $-3 < \dot{\theta} < 3$; for each initial condition Eq. (3) was integrated numerically for thirty drive cycles to allow the initial transient to decay, and the time-average angular velocity $\bar{\dot{\theta}}$ was computed for the following ten cycles. The distribution of $\bar{\dot{\theta}}$ reliably allowed assignment as a positive or negative stable or metastable running mode. The set of initial conditions θ and $\dot{\theta}$ yielding positive modes constitutes the basin of attraction for this mode and is shaded in Fig. 2; the basin of attraction for the negative mode is white. For all four cases in Fig. 2 the basin boundaries are fractal sets as discussed below. Also shown in Fig. 2 are the Poincaré sections at drive phase $\omega_0 t = 0 \pmod{2\pi}$ of the stable attractors for the two running modes, shown as heavy dots or lines. The Poincaré sections of two unstable period-3 orbits which lie on the basin boundary are shown as small open circles in Figs. 2(c) and 2(d).

Examination of Figs. 2(c) and 2(d) shows a development of both the Poincaré sections of the stable attractors and the basin boundaries characteristic of an interior crisis.[4] A pair of stable periodic running modes is produced by a saddle-node bifurcation at $g = 1.4919$; as g increases the two stable orbits become chaotic, but remain separate, each lying entirely within its basin as shown in Fig. 2(c). An interior crisis occurs between Figs. 2(c) and 2(d) at which the two unstable period-3 orbits on the basin boundary collide with the stable period-3 chaotic attractors. At this point the two modes lose their separate identity and join to form a

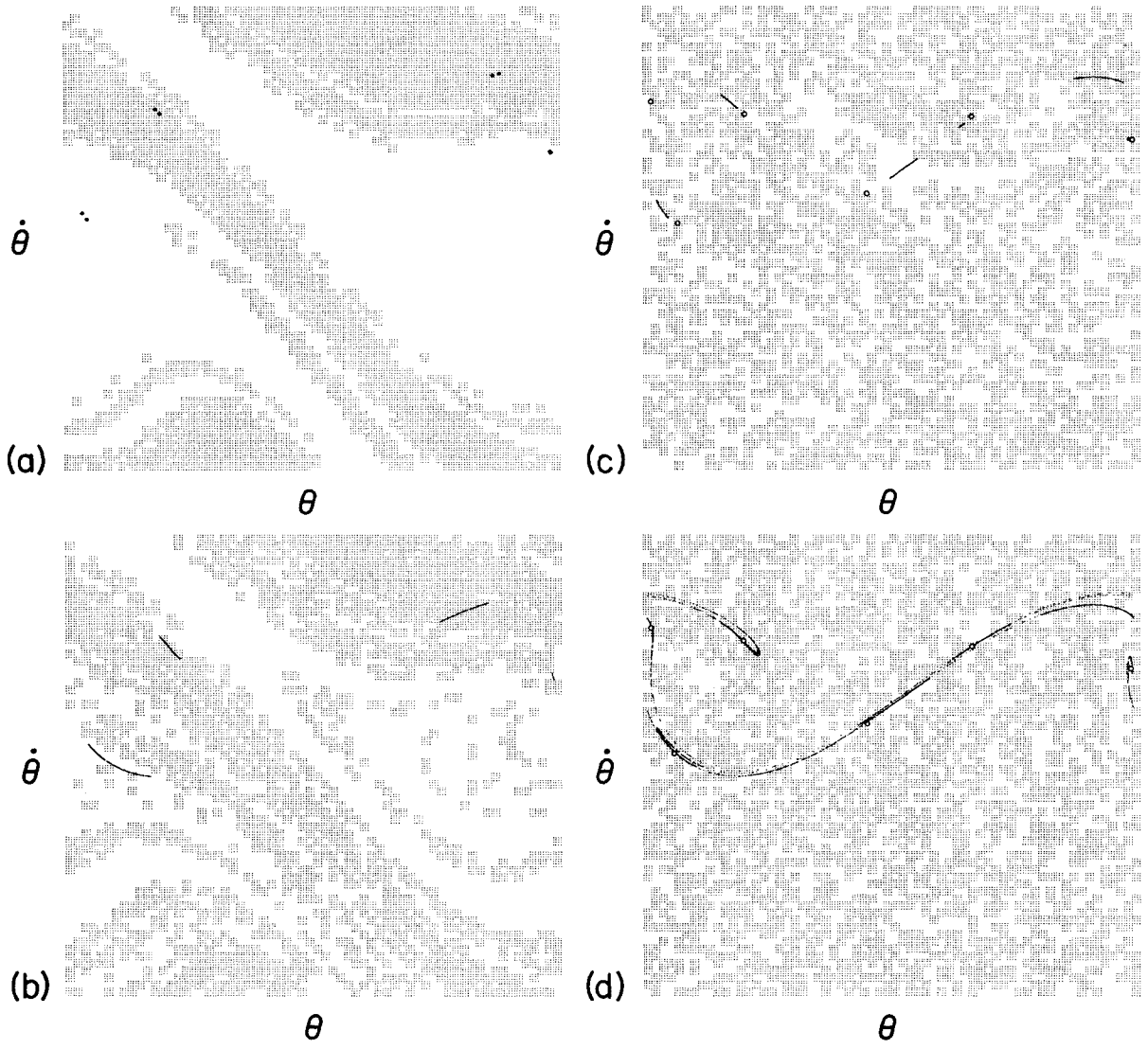

FIG. 2. Basins of attraction in angle θ (range 0 to 2π) and angular velocity $\dot{\theta}$ (range -3 to 3) for positive (shaded) and negative (blank) stable or metastable running modes computed from Eq. (3) for $\omega_0=\frac{2}{3}$, $Q=2$, and drive amplitudes (a) $g=1.4600$, (b) $g=1.4800$, (c) $g=1.4954$, and (d) $g=1.4955$ (see text). Also shown are Poincaré sections of the attractors (solid circles) in (a) to (d) and unstable orbits (open circles) in (c) and (d) at phase $\omega_0 t=0$ (mod2π).

folded chaotic attractor shown in Fig. 2(d). The basins of attraction also cease to exist separately, although one can reliably compute separate metastable basins as in Fig. 2(d). Pomeau-Manneville type-1 intermittency presumably occurs for parameter values near the saddle-node bifurcation which produces the two sets of stable and unstable period-3 orbits shown in Fig. 2(c).

The computed return maps θ_{n+3} vs θ_n for the two chaotic period-3 Poincaré sections shown in Fig. 2(c) each consist of three nearly one-dimensional parabolic segments which cross the diagonal $\theta_{n+3}=\theta_n$. The measured scaling of the average time $\bar{\tau}$ in each metastable running mode for $g>g_c$ is $1/\bar{\tau}\propto(g-g_c)^{\nu}$ with $\nu\simeq 0.5\pm 0.15$ in agreement with both models, Eqs. (1) and (2), in the quasi-one-dimensional case.

Far from the crisis, in Figs. 2(a) and 2(b), the basin boundaries display folding characteristic of chaotic systems, yet remain relatively simple. A striking increase in complexity is shown in Figs. 2(c) and 2(d) near the crisis at g_c as the folding evident in Figs. 2(a) and 2(b) evolves into complex structures resembling random white noise in θ and $\dot{\theta}$. The computed[26] dimension d of the basin boundaries for Figs. 2(a) to 2(d), respectively, is $d=1.63$, $d=1.88$, $d=1.97$, and $d=1.98$; for white noise $d=2$. Fractional dimensions $d>1$ imply that the basin boundaries possess structure on arbitrarily small scales in θ and $\dot{\theta}$ and raise questions about the functional form of low-frequency power

spectra and the influence of external noise.

We repeated the simulations above including an added random-noise term $\delta g(t)$ in Eq. (3) with a flat power spectrum. The effect of noise is to produce elongation of the Poincaré sections along directions for which the flow toward the attractor is slowest or divergent (chaotic), yielding orbits similar in appearance to intrinsic chaos shown for two different cases in Figs. 2(b) and 2(c). Well below the crisis at g_c the finite minimum separation of the attractor and the basin boundary requires a finite noise-induced excursion ϵ in θ and $\dot{\theta}$ to create extrinsic intermittency. When the basin boundaries are relatively simple, as in Fig. 2(a), and the fractal dimension is well below 2, extrinsic intermittency is not easily produced. For drive amplitudes g closer to g_c, shown in Figs. 2(b) and 2(c), the basin boundaries are complex with dimension $d \simeq 2$, and this minimum excursion approaches zero. In this case extrinsic intermittency is easily induced by very small amounts of external noise $\delta g(t)$. When present, intrinsic intermittency is surprisingly insensitive to physically reasonable noise levels. The power spectrum just above the crisis in Fig. 1(b) remained essentially unchanged until the rms noise amplitude averaged over Q drive cycles exceeded $\delta g_{\rm rms} \simeq 1.4 \times 10^{-5}$; a further increase in noise produced a flat power spectrum below a corner frequency which increased with external noise to $\omega \simeq 0.1\omega_0$ for $g_{\rm rms} \simeq 1.4 \times 10^{-2}$.

Both the functional form and noise scaling[5] of the noise-induced power spectrum can be estimated under the rather strong assumption that noise sufficiently modifies the attractor to produce a random sampling of phase space θ and $\dot{\theta}$. With this assumption the power spectrum is Lorentzian with a characteristic frequency equal to the noise-induced switching rate $1/\bar{\tau}$. Given a noise-induced perturbation of radius ϵ in θ and $\dot{\theta}$, the fraction f of initial conditions which yield uncertain steady states, and by assumption $1/\bar{\tau}$, scales as[5]

$$f \propto \epsilon^{2-d}. \tag{4}$$

In this picture, arbitrarily small excursions ϵ near the crisis at $g = g_c$ where $d \simeq 2$ produce a rapid noise-induced switching rate $1/\bar{\tau} \sim \omega_0$ which destroys both intrinsic stable and intermittent states. However, as shown above, neither the power-law functional form of the intrinsic power spectrum at the crisis nor the relative insensitivity to external noise agree with this picture. This implies that the locations of the attractors and the metastable basin boundary remain highly correlated until the noise amplitude becomes quite large.

We thank M. Beasley, E. Ott, J. Clarke, M. Tinkham, B. Mandelbrot, and R. Koch for helpful conversations. This work was supported by the U. S. Office of Naval Research, Contract No. N00014-84-K-0329. One of us (E.G.G.) also acknowledges receipt of an AT&T Bell Laboratories scholarship.

[1]Reviewed by J.-P. Eckmann, Rev. Mod. Phys. **53**, 643 (1981).

[2]Y. Pomeau and P. Manneville, Commun. Math. Phys. **74**, 189 (1980); P. Manneville, J. Phys. (Paris) **41**, 1235 (1980).

[3]J. E. Hirsch, B. A. Huberman, and D. J. Scalapino, Phys. Rev. A **25**, 519 (1982).

[4]C. Grebogi, E. Ott, and J. A. Yorke, Phys. Rev. Lett. **48**, 1507 (1982), and **50**, 935 (1983), and Physica (Utrecht) **7D**, 181 (1983).

[5]C. Grebogi, S. W. McDonald, E. Ott, and J. A. Yorke, Phys. Lett. **99A**, 415 (1983).

[6]I. Procaccia and H. Schuster, Phys. Rev. A **28**, 1210 (1983).

[7]T. Geisel and S. Thomae, Phys. Rev. Lett. **52**, 1936 (1984); T. Giesel, J. Nierwetberg, and A. Zacherl, Phys. Rev. Lett. **54**, 616 (1985).

[8]G. Mayer-Kress and H. Haken, Physica (Utrecht) **10D**, 329 (1984).

[9]F. T. Arecchi, R. Badii, and A. Politi, Phys. Lett. **103A**, 3 (1984), and to be published.

[10]B. A. Huberman, J. P. Crutchfield, and N. H. Packard, Appl. Phys. Lett. **37**, 750 (1980).

[11]R. L. Kautz, J. Appl. Phys. **52**, 3528, 6241 (1981).

[12]N. F. Pederson and A. Davidson, Appl. Phys. Lett. **39**, 830 (1981).

[13]D. D'Humieres, M. R. Beasley, B. A. Huberman, and A. Libchaber, Phys. Rev. A **26**, 3483 (1982).

[14]W.J. Yeh and Y. H. Kao, Appl. Phys. Lett. **42**, 299 (1983).

[15]H. Seifert, Phys. Lett. **98A**, 213 (1983).

[16]H. Koga, H. Fujisaka, and M. Inoue, Phys. Rev. A **28**, 2370 (1983).

[17]M. Octavio, Phys. Rev. B **29**, 1231 (1984).

[18]I. Goldhirsch, Y. Imry, G. Wasserman, and E. Ben-Jacob, Phys. Rev. B **29**, 1218 (1984).

[19]E. G. Gwinn and R. M. Westervelt, in *Proceedings of the Seventeenth International Conference on Low-Temperature Physics, Karlsruhe, West Germany, 1984,* edited by U. Eckern, A. Schmid, W. Weber, and H. Wuhl (North-Holland, Amsterdam, 1984), p. 1139.

[20]R. F. Miracky, M. H. Devoret, and J. Clarke, to be published.

[21]R. F. Miracky, J. Clarke, and R. H. Koch, Phys. Rev. Lett. **50**, 856 (1983).

[22]V. N. Gubankov, K. I. Konstantinyan, V. P. Koshelets, and G. A. Ovsyannikov, IEEE Trans. Magn. **19**, 637 (1983).

[23]M. Octavio and C. Readi Nasser, Phys. Rev. B **30**, 1586 (1984).

[24]Q. Hu, J. U. Free, M. Iansiti, O. Liengme, and M. Tinkham, in Proceedings of the Applied Superconductivity Conference, 1984 (to be published).

[25]B. B. Mandlebrot, *The Fractal Geometry of Nature* (Freeman, San Francisco, 1983), and references therein.

[26]P. Grassberger and I. Procaccia, Phys. Rev. Lett. **50**, 346 (1983); this method determines the correlation exponent which is a good approximation to the Hausdorff dimension of fractal sets such as the basin boundary.